Role of hydrogen bonding in the oxidation potential of enols

Mukul Lal,[1] Anja Langels,[2] Hans-Jörg Deiseroth,[3] Jens Schlirf[3] and Michael Schmittel[1]*

[1]FB 8 (Chemie-Biologie), Organische Chemie I, Universität Siegen, Adolf-Reichwein-Strasse, D-57068 Siegen, Germany
[2]Institut für Organische Chemie der Universität Würzburg, Am Hubland, D-97074 Würzburg, Germany
[3]FB 8 (Chemie-Biologie), Anorganische Chemie I, Universität Siegen, Adolf-Reichwein-Strasse, D-57068 Siegen, Germany

epoc ABSTRACT: Three stable β,β-dimesityl enols with heteroaromatic rings in the α-position were synthesized to study the effect of OH$\cdots$N hydrogen bonding on the oxidation potentials of enols. In contrast to its solid-state structure, enol **E1** exists predominantly as intramolecularly hydrogen-bonded species in solution. For enol **E2** an intermolecular hydrogen bond and for E3 a partial proton transfer were established based on NMR, dilution experiments, solvent dependence and UV–visible spectroscopic studies. Cyclic voltammetric investigations revealed that OH$\cdots$N hydrogen bonding may shift the oxidation potentials of enols by up to 510 mV cathodically. Copyright © 2003 John Wiley & Sons, Ltd.

Additional material for this paper is available from the epoc website at http://www.wiley.com/epoc

KEYWORDS: enols; redox potential; hydrogen bonding; oxidation

INTRODUCTION

With our ongoing efforts to understand and develop radical ion probes that would trap radical ionic intermediates[1] such as biologically relevant enol radical cations directly during enzymatic action, we became interested to know the extent to which hydrogen bonding, a common motif for the stabilization of reactants, intermediates and products in the active site of the enzyme, would alter the redox potential of bound substrates.

Enol and enol ether radical cations have been extensively investigated for their role in DNA damage.[2,3] Moreover, they have been invoked in a number of important biological transformations carried out by coenzyme B$_{12}$-dependent enzymes.[4,5] The two main reactions that determine the fate of the enol radical cation are either single electron transfer reduction or deprotonation leading to an α-carbonyl radical (Scheme 1).[6,7]

Hydrogen bonding to enol radical cations should not only reduce their reduction potential but also enhance the deprotonation step generating α-carbonyl radicals. Hence the modulation of the reactivity of the enol radical cation intermediate in the active site through hydrogen bonding becomes crucial for the mode of action.

In the last 20 years, knowledge about the synthesis and structures of isolable and stable simple enols[8] has steadily increased.[9,10] Two different types of substituents, halo-

gens and sterically bulky aryl groups, have found widespread use in stabilizing enols and rendering them isolable. We chose the sterically encumbered mesityl group as the basis of enols **E1–E3** and decided to investigate their hydrogen bonding characteristics and one-electron oxidation chemistry.

RESULTS AND DISCUSSION

Enols **E1–E3** were prepared by the reaction of β,β-dimesitylketene[8] with the corresponding heteroaryl lithium reagent, in yields ranging from 24 to 40%. They were fully characterized by ^{1}H and ^{13}C NMR, IR and elemental analysis. Moreover, the solid-state structure of **E1** (see below) confirms the enol structure of **E1–E3**.
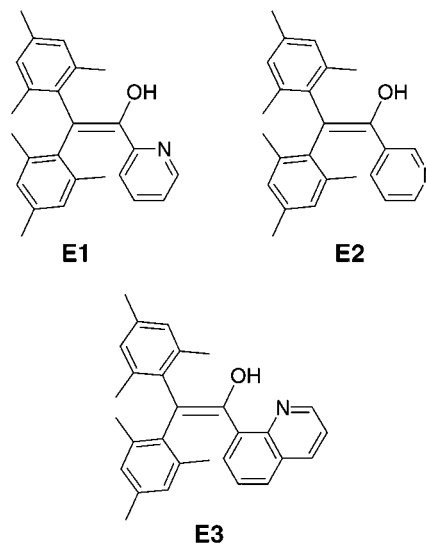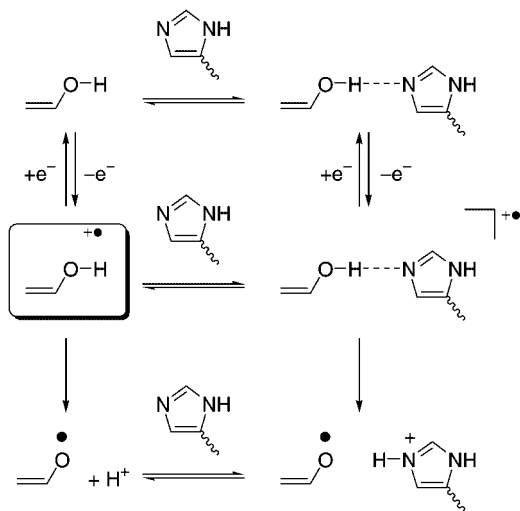
Scheme 1. Modulation of the enol radical cation reactivity through hydrogen bonding

Hydrogen bonding in solution

The shift of O*H* signals (δ_{OH}) in the ^{1}H NMR spectra can be a diagnostic tool to check for inter- and intramolecular hydrogen bonding.[11] NMR experiments on **E1** in deuterated chloroform showed no shift in enol O*H* even at 1000-fold dilution, clearly indicative of intramolecular hydrogen bonding (Table 1). Similarly, no shift was observed for **E3** (100-fold dilution), whereas **E2** exhibited a notable high-field shift δ_{OH} of 0.5 ppm. In summary, this argues for intramolecular hydrogen bonding for **E1** and **E3**, but intermolecular hydrogen bonding between two molecules of **E2** in CDCl$_3$ at least at higher concentration. In DMSO-d_6, a much stronger hydrogen-bond acceptor solvent than CDCl$_3$, **E2** showed no shift in enol O*H* even at 1000-fold dilution. Apparently, in DMSO the intermolecular (**E2**)OH$\cdots$N(**E2**) hydrogen bond is replaced by a (**E2**)OH$\cdots$O=SMe$_2$ interaction.

Although the NMR dilution experiments are convincing about intramolecular hydrogen bonding in **E1** and **E3**, one still has to differentiate between N$\cdots$HO hydrogen bonding and the Mes(π)$\cdots$HO interaction. Moreover, the large upfield shift δ_{OH} of **E3** (11 ppm) vs δ_{OH} of **E1** (8.4 ppm) requires further experiments, such as solvent dependence studies.

Table 1. δ_{OH} values (ppm) for enols **E1**–**E3** upon dilution in CDCl$_3$

Dilution factor	δ_{OH}(**E1**)	δ_{OH}(**E2**)	δ_{OH}(**E3**)
0	8.44[a]	5.69[b]	11.09[c]
10	8.43	5.31	11.08
100	8.42	5.24	11.05
1000	8.42	5.21	—

[a] Initial concentration: 0.14 M.
[b] Initial concentration: 0.10 M.
[c] Initial concentration: 0.06 M.

Table 2. δ_{OH} values (ppm) for enols **E1**–**E3** in different solvents

Solvent	δ_{OH}(**E1**)	δ_{OH}(**E2**)	δ_{OH}(**E3**)
CD$_2$Cl$_2$	—	5.41	—
CDCl$_3$	8.44	5.26	11.09
C$_6$D$_6$	8.92	5.29	11.21
Diethyl ether-d_{10}	—	5.53	—
Acetone-d_6	8.55	7.64	10.71
THF-d_8	—	7.70	—
DMF-d_7	8.87	9.11	10.35
DMSO-d_6	8.75	8.80	9.83

It is known from Rappoport and co-workers' work[12] that δ_{OH} of triarylenols shifts downfield when the solvent polarity and the solvent hydrogen bond acceptor ability are increased. This was interpreted on the basis that in non-polar non-hydrogen bond accepting solvents the enol unit adopts a synperiplanar conformation that is stabilized by an OH$\cdots$(π)Mes interaction. In hydrogen bond accepting solvents the enol unit assumes an anticlinal conformation allowing for interaction with the solvent. Of the enols in our study, only **E2** (Table 2) exhibits an analogous correlation to Mes$_2$C=C(OH)Ph.[12a] On the other hand, **E2** shows concentration-dependent δ_{OH} in CHCl$_3$ but not in DMSO. As a consequence, an appreciable amount of **E2**–**E2** interaction can exist in non-polar solvents, but in more polar solvents the **E2**–**E2** interaction is replaced by a hydrogen bond to the solvent.

E1 and **E3** show completely different behavior. In line with expectations for intramolecular OH$\cdots$N hydrogen bonding, **E1** exhibited a small (and random) shift δ_{OH} when the solvent polarity was increased. In contrast, **E3** exhibited a small but regular upfield shift δ_{OH} with increasing solvent polarity (11.09 in CDCl$_3$; 9.83 in DMSO-d_6) that correlated linearly with the dielectric constant of the solvents used (Fig. 1). The inverse relationship suggests an intramolecular hydrogen bond with strong zwitterionic character for **E3**, thus explaining
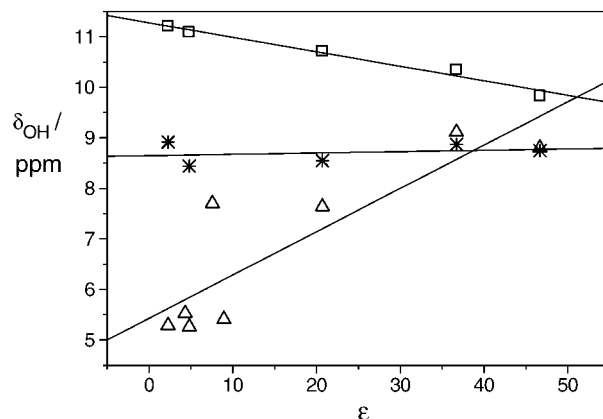

Figure 1. Plot of δ_{OH} values (ppm) versus the dielectric constant of the solvent for enols **E1** ($*$), **E2** ($\triangle$) and **E3** ($\square$)

convincingly the large difference in δ_{OH} for the two enols **E3** and **E1**.

The zwitterionic character of **E3** is further confirmed by the UV–visible spectroscopic results (dichloromethane). **E3** exhibits an absorption band with $\lambda_{max} = 379$ nm, which is much more bathochromically shifted than that of **E1** ($\lambda_{max} = 320$ nm), **E2** ($\lambda_{max} = 340$ nm) or quinoline ($\lambda_{max} = 313$ nm). Comparison with the *N*-protonated **E3** + H$^+$ ($\lambda_{max} = 433$ nm) indicates that proton transfer in **E3** is not complete. The zwitterionic character of **E3** is additionally confirmed by a hypsochromic shift in the following series: benzene ($\lambda_{max} = 391$ nm), chloroform ($\lambda_{max} = 381$ nm), acetone ($\lambda_{max} = 379$ nm), DMSO ($\lambda_{max} = 368$ nm).

In summary, the three different model compounds constitute three different H-bonded enolic systems. **E1** forms an intramolecular hydrogen bond as depicted in **E1'**, **E2** is involved in an intermolecularly hydrogen bonded dimer **E2'** and **E3** shows an intramolecular hydrogen bond with partial proton transfer (as in **E3'**). While it is well known that sterically shielded enols of the Fuson type cannot form OH···OH bonded dimers[13] owing to steric constraints, molecular modeling on **E2'** showed that the OH–pyridine bonded dimeric structure does not bring about any significant steric repulsion.


E1'

E2'

E3'
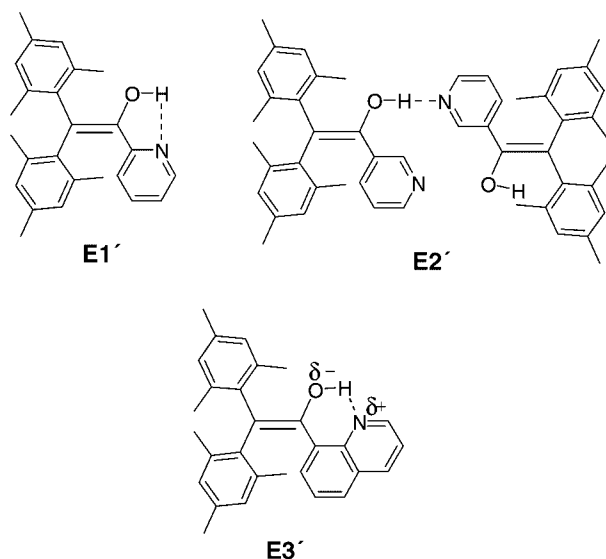
Hydrogen bonding in the solid state

In the solid state, **E1** crystallizes in the space group *P*-1 (triclinic) with one formula unit in the asymmetric unit (all atoms placed on general position 2*i*, Fig. 2). Intermolecular hydrogen bonding was observed in the solid state leading to a dimer with OH as the hydrogen bond donor and the nitrogen of the pyridine ring as the acceptor. The H···N distance was found to be 192 pm (Fig. 3). Some of the important bond distances and bond angles are summarised in Table 3.
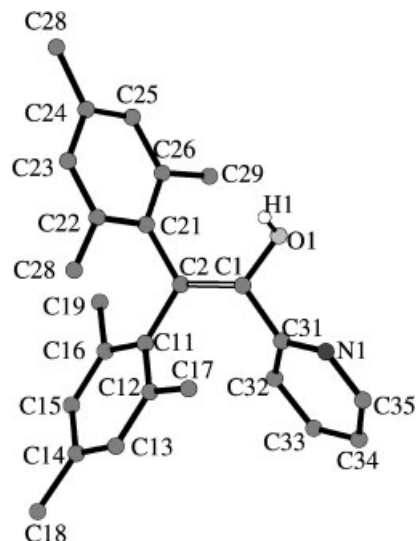
Figure 2. Stick ball representation of **E1** from the x-ray structure analysis
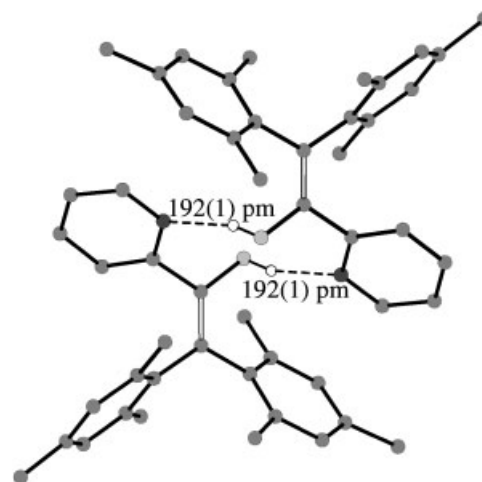
Figure 3. Reduced projection of **E1** showing a dimeric arrangement formed by intermolecular hydrogen bonding

Table 3. Selected bond distances (pm) and angles (degrees) of **E1**

O1—H1	82.0(4)
H1···N1	191.9(10)
O1···N1	271.1(15)
C11—C2—C1	120.16(1)
C21—C2—C1	119.99(1)
O1—C1—C2—C21	3.94(2)
C1—C2—C21—C22	−126.54(1)
C2—C1—C31—N1	−133.38(1)
O1—H1···N1	162.09(2)
C31—C1—C2	124.28(1)
O1—C1—C2	124.99(1)
C11—C2—C1—C31	8.33(2)
C1—C2—C11—C16	−123.10(1)
H1—O1—C1—C2	48.15(2)

E1-E3   **R1-R3**   **B1-B3**

Scheme 2
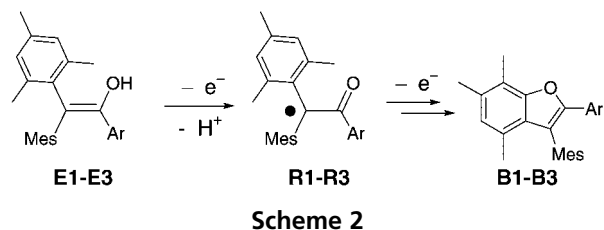
Table 4. Oxidation potentials of enols **E1**–**E3** obtained from cyclic voltammetry in acetonitrile (dichloromethane) at a scan rate of $100\,mV\,s^{-1}$

| Enol	E_{pa} (I) (V_{Fc})	E_{pa} (II) (V_{Fc})	E_{pa} (III) (V_{Fc})
E1	0.46 (0.53)	—	1.20 (1.15)
E2	0.36 (0.34)	0.76 (0.76)	1.04 (1.02)
E3	0.02 (0.04)	0.27 (0.25)	0.80 (0.78)

Cyclic voltammetric investigations

It is known that the oxidation of β,β-dimesityl enols furnishes the benzofuran derivatives (Scheme 2).[7,14,15] Hence two oxidation waves are typically expected in cyclic voltammetric experiments for β,β-dimesityl enols, the first wave of which (irreversible) is assigned to the enol oxidation and the other (often partially reversible) wave at higher potential corresponds to the oxidation of the benzofuran derivative.[16] Here, we will only concentrate on the enol oxidation waves.

Cyclic voltammograms in acetonitrile and dichloromethane were measured for **E1**–**E3** (Fig. 4). For all systems more than one oxidation wave is observed. We analyzed the first oxidation wave for each enol using the Shain–Nicholson[17] criterion ($I_{pa}/v^{1/2}$ vs v), revealing an EC_{irr} mechanism for **E1** and **E2** and an EC_{rev} mechanism for **E3**.

For **E1** two irreversible oxidation waves appeared at a $100\,mV\,s^{-1}$ scan rate. Acid addition in dichloromethane shifted the oxidation wave from $E_{pa} = 0.53$ to 0.75–0.77 V_{Fc} (at 20 equiv. of trifluoroacetic acid). In addition, a new wave was observed at $E_{pa} = 0.91\,V_{Fc}$ that finally merged with wave III. Addition of 0.5 equiv, of pyridine led to the complete disappearance of wave III.

For **E2** three oxidation waves were observed starting from $E_{pa} = 0.36$ (0.34), 0.76 (0.76) and 1.04 (1.02) V_{Fc} in acetonitrile (dichloromethane) (a closer inspection of the first oxidation wave in **E2** indicates that it is superimposed by a small, slightly cathodically shifted wave; concentration- and temperature-dependent cyclic voltammetric studies indicated that this wave is due to a second dimer of **E2**). Upon dilution of **E2** in dichloromethane the peak current of the oxidation wave at 0.34 V_{Fc} decreased (a slight shift towards higher oxidation potential was
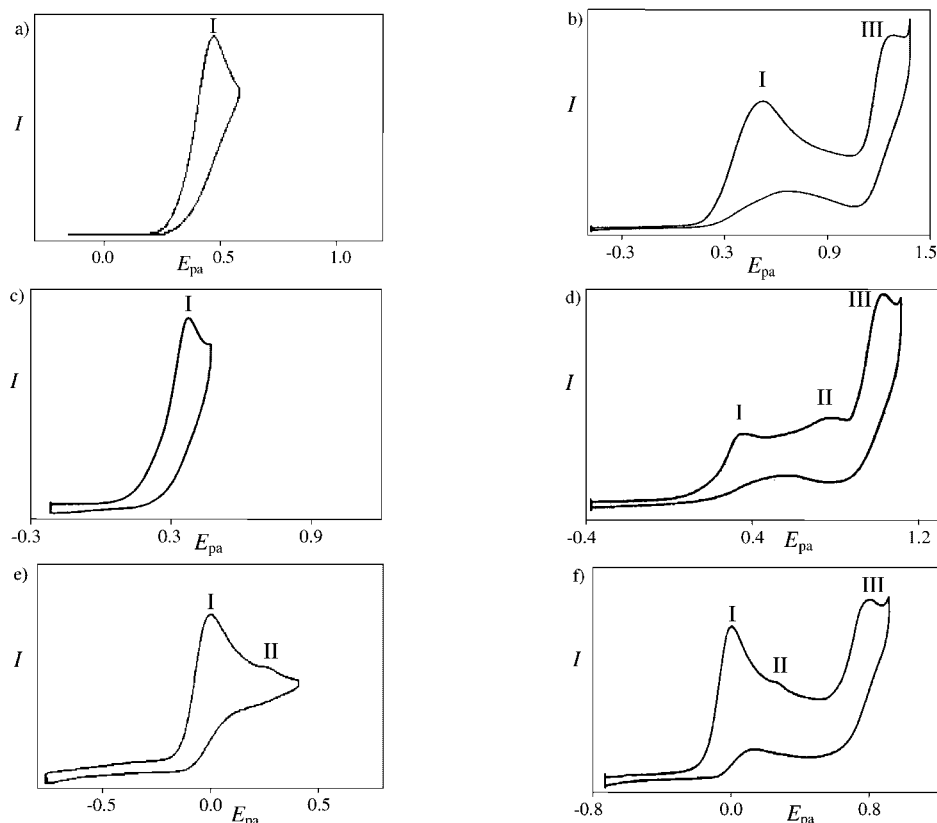
Figure 4. Cyclic voltammograms of enols **E1** (a, b), **E2** (c, d) and **E3** (e, f) at a scan rate of $100\,mV\,s^{-1}$ in acetonitrile. The left cyclic voltammogramms (a, c, e) show only the oxidation wave [E_{pa} (V)] of the hydrogen-bonded enol, the right ones (b, d, f) all waves in the spectrum that pertain also to enol oxidation (see Discussion)

additionally registered), whereas the intensities of the other waves ($E_{pa} = 0.76$ and $1.02\,V_{Fc}$) remained unchanged.

The cyclic voltammogram of **E3** showed three waves in acetonitrile (or dichloromethane) at a $100\,mV\,s^{-1}$ scan rate. Dilution experiments in dichloromethane indicate no change in the intensity ratios of the waves at 0.04 and 0.25 V. After addition of trifluoroacetic acid, the waves at 0.02 V and $0.25\,V_{Fc}$ completely disappeared. No change for the wave at $E_{pa} = 0.78\,V_{Fc}$ was observed. In contrast, addition of 0.5 equiv., of pyridine led to the complete disappearance of wave III.

The assignment of the waves becomes straightforward on the basis of the above results. For all three systems, the lowest $E_{pa} = 0.46\,V_{Fc}$ (**E1**), $0.36\,V_{Fc}$ (**E2**) and $0.02\,V_{Fc}$ (**E3**) corresponds to the oxidation of the hydrogen bonded enols **E1'–E3'**. The waves at $E_{pa} = 1.20$ (**E1·H$^+$**), 1.04 (**E2·H$^+$**) and $0.80\,V_{Fc}$ (**E3·H$^+$**) were assigned to the oxidation of the N-protonated enols **E·H$^+$** based on the acid and base addition experiments.

With all these assignments being straightforward, the origin of the waves at $E_{pa} = 0.76\,V_{Fc}$ (in dichloromethane $0.76\,V_{Fc}$) and $0.27\,V_{Fc}$ ($0.25\,V_{Fc}$) in **E2** and **E3** remains unclear. As both waves show up more clearly on raising scan rate, one is led to suggest that they belong to the non-hydrogen-bonded enols. These enols may be present as minor components in a slow equilibrium with **E2'** and **E3'**. To elucidate this question we sought a way to approximate the oxidation potential of the non-hydrogen-bonded enols **E1–E3**. In principle, one should be able to estimate the oxidation potential of enols **E1–E3** from their adiabatic ionization potentials. Since the oxidation potentials of a number of β,β-dimesityl enols with α-aryl substituents had been previously measured in our laboratory, we determined their adiabatic ionization potentials

Table 5. Adiabatic ionization potentials of various enols obtained by AM1 calculation and their experimentally obtained oxidation potentials in acetonitrile
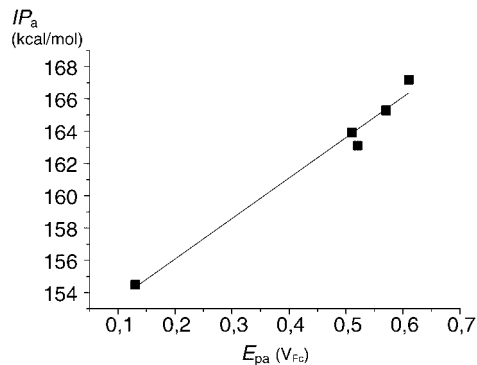
Mes$_2$C=C(OH)R	IP_a (kcal mol^{-1})	E_{pa} (V$_{Fc}$)
R = phenyl	167.2	0.61
R = p-tolyl	165.3	0.57
R = p-anisyl	163.1	0.52
R = 3,4-dimethoxyphenyl	163.9	0.51
R = 4-N,N-dimethylaminophenyl	154.5	0.13

Figure 5. Plot of experimentally obtained oxidation potentials E_{pa} for enols (in acetonitrile) versus the calculated IP_a by AM1 ($r^2 = 0.98$)

IP_a by AM1 calculations [a comparison of calculated and experimental ionization energies shows that semiempirical calculations work better for ionization potentials than *ab initio* (STO-3G, 3–21G, 6–31G*, 6–31+G**) and DFT (B3PW91, BLYP, B3LYP, B3P86, B3P86) calculations][18] and established a correlation with their E_{pa} in solution (Table 5, Fig. 5).

As a good linear correlation [IP_a (kcal mol^{-1}) $= 25.1E_{pa}$ (V$_{Fc}$) $+ 151.05$, $r^2 = 0.98$] (1 kcal = 4.184 kJ) between the adiabatic ionization potential and the oxidation potential was observed for a small series of aryl enols, this should allow one to make a reliable prediction for the oxidation potential of **E1–E3** when the enols are not involved in hydrogen bonding but in an $OH\cdots(\pi)$Mes interaction. Hence, from the adiabatic ionization potentials of **E1–E3** [in the lowest energy $OH\cdots(\pi)$Mes conformation] and the above correlation, the expected E_{pa} for the non-hydrogen-bonded enols were determined (Table 6). When these E_{pa} are compared with that of the phenyl-substituted enol (Table 5, $E_{pa} = 0.61\,V_{Fc}$) it becomes evident that the E_{pa} of enols **E1–E3** (exchange of phenyl by heteroaryl groups) is little influenced by inductive or conjugative effects.

With E_{pa} for the non-hydrogen-bonded enols at hand, we examined whether their oxidation waves are detectable in the cyclic voltammetric investigations. Indeed, the additional wave at $E_{pa} = 0.76\,V_{Fc}$ (**E2**, wave II) may correspond to the oxidation of the non-hydrogen-bonded enols **E2**. Such an assignment can be checked as the intermolecular dimer should break down upon dilution; indeed, upon dilution the wave at $0.76\,V_{Fc}$ increased on

Table 6. AM1-calculated and experimental oxidation potentials E_{pa} (in acetonitrile) of **E1–E3**

Enol	ΔH_f° (enol) (kcal mol^{-1})	ΔH_f° (enol$^+$) (kcal mol^{-1})	IP_a (kcal mol^{-1})	E_{pa} (V$_{Fc}$)^a without $OH\cdots N$	E_{pa} (V$_{Fc}$)^b with $OH\cdots N$
E1	41.2	211.1	169.9	0.75	0.46
E2	38.1	208.6	170.5	0.78	0.36
E3	61.7	226.0	164.3	0.53	0.02

[a] Calculated from IP_a.
[b] Experimental data for comparison; see also Table 4.

expense of the wave at 0.36 V_{Fc}. For **E3** the situation is less clear, as the enol should only exist without the strong OH···N hydrogen bonding if a kinetically locked s-*anti* conformation at the enol–quinoline bond is possible. AM1 calculations, however, only revealed a small barrier for rotation, so that the wave at 0.25 V_{Fc} (**E3**, wave II) should not correspond to the oxidation of the non-hydrogen bonded enol, but may be to the protonated α-carbonyl radical **R3** (some of the α-carbonyl radicals have proved to be stable for hours).[19]

What is the effect of hydrogen bonding on the oxidation potential? First, we have to realize that E_{pa} depend on the kinetics of the follow-up deprotonation (EC_{irr}). Because for enol radical cations the deprotonation rate constants[20] and hence the kinetic contributions to the potential are similar, we may use E_{pa} instead of the thermochemically relevant $E_{1/2}$ for the ensuing analysis. The data in Table 6 suggest that the cathodic shift through hydrogen bonding can amount to a few hundred millivolts. As one would expect, the $\Delta\Delta E_{pa}^{H} = \Delta E_{pa}$ (free enol) $- \Delta E_{pa}$ (H-bonded enol) is more pronounced for **E3** ($\Delta\Delta E_{pa}^{H} = 510$ mV) than for **E1** ($\Delta\Delta E_{pa}^{H} = 290$ mV) because the geometric situation in a six-membered ring is more favorable for hydrogen bonding than in a five-membered ring. On the other hand, inter-molecular hydrogen bonding in **E2** accounts for $\Delta\Delta E_{pa}^{H} = 420$ mV.

CONCLUSION

Hydrogen bonding can have a profound effect in altering the oxidation potentials of enols. In comparison, the oxidation potentials of hydrogen-bonded enols were 290–510 mV lower than those of the non-hydrogen-bonded enols.

From our investigations, it becomes clear that enol radical cations, putative intermediates in enzymatic reactions such as ribonucleotide reductase,[4] may be much weaker oxidants than expected from their solution redox potentials. Hydrogen bonding in the active site could easily shift the potential cathodically by several hundred millivolts, a fact that has to be taken into consideration when new radical ion probes are designed.

EXPERIMENTAL

Commercial reagents were purchased from standard chemical suppliers and were used without further purification. Dimesitylketene was prepared as described in Ref. 21. The one-electron oxidation reactions were carried out in acetonitrile which was of HPLC quality (Riedel-de Haën) and distilled from P_2O_5. Melting-points were recorded with a Büchi Smp-20 apparatus. Infrared spectra were measured with a Perkin-Elmer 1605 FT-IR infrared spectrophotometer. ^{1}H NMR spectra [Bruker AC 200 (200 MHz)] and ^{13}C NMR spectra [Bruker AC 200 (50 MHz)] are referenced to tetramethylsilane; coupling constants are provided in hertz. The single crystal measurement was carried out on a STOE IPDS one-circle image-plate diffractometer equipped with an Oxford Cryostream liquid nitrogen cooling device. Further details on measurement, refinement and crystal data are summarized in Table 1 in the Supplementary Material. The coordinates of the hydrogen atoms were placed and refined for idealized geometries with isotropic displacement. The crystal structure solution and refinement based on F^2 were performed by direct methods and subsequent Fourier syntheses with anisotropic displacement parameters for all non hydrogen atoms using SHELXS-97 and SHELXL-97.[22] Theoretical calculations on enol and enol radical cations were performed at the AM1 level using Spartan, and only those structures in enols and enol radical cations which had lowest heat of formation and no hydrogen bonding were used for calculating the adiabatic ionisation potential. Cyclic voltammetry was performed on a Model 362 potentiostat (Princeton Applied Research) and recorded with the help of an *x,y* recorder (Model PM 8271, Philips). The electrochemical cell was equipped with a platinum disc (1.0 mm diameter) working electrode, a platinum auxiliary electrode and a silver wire as reference electrode. Ferrocene was used as internal reference.

*2,2-Dimesityl-1-(2-pyridyl)ethenol (**E1**).* To a solution of 2-bromopyridine (330 µl, 545 mg, 3.43 mol) in dry THF (20 ml) at −78 °C, n-butyllithium (2.5 M in n-hexane, 1.22 ml, 3.7 mmol) was added dropwise. After 10 min a solution of dimesitylketene (960 mg, 3.43 mmol) in dry THF (20 ml) was added. The reaction mixture was stirred for 2 h at −78 °C and 12 h at room temperature. After quenching with saturated aqueous. NH_4Cl solution (20 ml) and extraction with Et_2O (3 × 20 ml), the combined organic layers were dried (Na_2SO_4). The solvent was removed *in vacuo* and the remaining brown oil was chromatographed on silica gel [hexane–diethyl ether (1:1), $R_f = 0.6$] yielding the desired enol **E1** (350 mg, 1.0 mmol, 29%) as a white solid. **E1**: m.p. 168–170 °C. IR (KBr): $\tilde{\nu} = 3314$ cm^{-1} (bm, O–H), 2918 (C–H), 2851 (m), 1609 (m), 1590 (s), 1564 (m), 1462 (s), 1436 (s), 1368 (m), 1276 (m), 1252 (m), 1197 (m), 1151 (m), 1084 (m), 900 (m), 856 (s). ^{1}H NMR (CDCl$_3$, 200 MHz): $\delta = 1.99$, 2.15 and 2.27 (3s, coalescence, 18 H, Mes-CH$_3$), 6.79 (s, 2 H, Mes-H), 6.85 (s, 2 H, Mes-H), 6.91 (d, 1 H, $J = 7.8$, 3'-H), 7.12 (m, 1 H, 5'-H), 7.35 (dt, 1 H, $J = 7.8$, $J = 1.7$, 4'-H), 8.44 (bs, 1 H, OH), 8.53 (d, 1 H, $J = 4.7$, 6'-H) ^{13}C NMR (CDCl$_3$, 63 MHz): $\delta = 20.83$, 20.89, 20.95, 21.07, 114.83, 122.53, 129.09, 129.59, 129.73, 134.68, 135.55, 136.02, 136.10, 136.51, 138.11, 138.42, 146.35, 147.41, 153.09. Elemental analysis: $C_{25}H_{27}ON$ (357.50) calcd C 83.99, H 7.61, N 3.92; found C 83.86, H 7.57, N 3.92%.

*2,2-Dimesityl-1-(3-pyridyl)ethenol (**E2**).* To a solution of 3-bromopyridine (300 μl, 492 mg, 3.4 mol) in dry THF (20 ml) at −78 °C, n-butyllithium (2.5 M in n-hexane, 1.2 ml, 3.7 mmol) was added dropwise. After 10 min a solution of dimesitylketene (960 mg, 3.43 mmol) in dry THF (20 ml) was added. The reaction mixture was stirred for 2 h at −78 °C and 12 h at room temperature. After quenching with saturated aqueous NH_4Cl solution (20 ml) and extraction with Et_2O (3 × 20 ml) the combined organic layers were dried (Na_2SO_4). The solvent was removed *in vacuo* and the remaining brown oil was chromatographed on silica gel [hexane–diethyl ether (1:1), $R_f = 0.2$] yielding the desired enol **E2** (400 mg, 1.12 mmol, 33%) as a white solid. **E2**: m.p. 196–198 °C. IR (KBr): $\tilde{v} = 3421$ cm^{-1} (bm, O–H), 2947 (C–H), 2919 (s), 2856 (m), 2617 (w), 1933 (vw), 1593 (s), 1560 (m), 1441 (s), 1155 (m), 1030 (s), 850 (s). ^{1}H NMR (CDCl$_3$, 200 MHz): $\delta = 1.91$, 2.19 and 2.27 (3s, coalescence, 18 H, Mes-CH$_3$), 5.61 (s, 1 H, OH), 6.68 (s, 2 H, Mes-H), 6.89 (bs, 2 H, Mes-H), 7.07 (dd, 1 H, $J = 7.9$, $J = 4.9$, 5′-H), 7.59 (dt, 1 H, $J = 7.9$, $J = 1.7$, 6′-H), 8.31 (dd, 1 H, $J = 4.9$, $J = 1.7$, 4′-H), 8.48 (d, 1 H, $J = 1.7$, 2′-H). ^{13}C NMR (CDCl$_3$, 63 MHz): $\delta = 21.68$, 21.77, 21.87, 114.27, 123.81, 130.64, 133.09, 133.47, 135.48, 136.72, 137.39, 138.19, 138.76, 139.89, 148.70, 149.67, 150.88. Elemental analysis: C$_{25}$H$_{27}$ON (357.50) calcd C 83.99, H 7.61, N 3.92%; found C 83.82, H 7.76, N 3.89%.

*2,2-Dimesityl-1-(8-quinolinyl)ethenol (**E3**).* To a solution of 8-bromoquinoline (0.5 g, 2.6 mmol) in dry THF (20 ml) at −78 °C, *sec*-butyllithium (2.5 M in n-hexane, 1.0 ml, 2.4 mmol) was added dropwise. After 10 min a solution of dimesitylketene (733 mg, 2.64 mmol) in dry THF (20 ml) was added. The reaction mixture was stirred for 2 h at −78 °C and 12 h at room temperature. After quenching with saturated aqueous NH_4Cl solution (20 ml) and extraction with Et_2O (3 × 20 ml), the combined organic layers were dried (Na_2SO_4). The solvent was removed *in vacuo* and the remaining brown oil was chromatographed on silica gel [hexane–diethyl ether (1:1), $R_f = 0.48$] yielding the desired enol **E3** (475 mg, 1.17 mmol, 44%) as an orange solid. **E3**: m.p. 206–208 °C. IR (KBr): $\tilde{v} = 3389$ cm^{-1} (bm, O–H), 2953 (C–H), 2917 (s), 2857 (m), 1956 (vw), 1613 (s), 1408 (m), 1372 (s), 1311 (m), 1189 (m), 1014 (s), 900 (m), 852 (s), 790 (s). ^{1}H NMR (DMSO-d_6, 400 MHz): $\delta = 1.75$, 2.05 and 2.21 (3s, coalescence, 18 H, Mes-CH$_3$), 6.54 (bs, 2 H, Mes-H), 6.77 (bs, 2 H, Mes-H), 7.28 (t, 1 H, $J = 8.0$, 3′-H), 7.38 (dd, 1 H, $J = 8.0$, $J = 1.4$, 6′-H), 7.57 (dd, 1 H, $J = 4.2$, $J = 8.4$, 7′-H), 7.86 (dd, 1 H, $J = 1.4$, $J = 8.0$, 5′-H), 8.41 (dd, 1 H, $J = 1.7$, $J = 8.4$, 4′-H), 8.90 (dd, 1 H, $J = 1.7$, $J = 4.2$, 1′-H), 9.84 (s, 1 H, OH). ^{13}C NMR (DMSO-d_6, 100 MHz): $\delta = 20.33$, 20.51, 114.41, 121.32, 125.72, 128.15, 128.55, 131.67, 134.22, 134.42, 135.72, 136.66, 137.24, 137.78, 145.54, 149.27, 151.17. Elemental analysis: C$_{29}$H$_{29}$ON (357.50) calcd C 85.47, H 7.17, N 3.44%; found C 85.76, H 7.22, N 3.52%.

Supplementary material

Details of the x-ray structure analysis and the cif file of **E1** are available at the epoc website at http://www.wiley.com/epoc.

REFERENCES

1. Schmittel M, Ghorai MK. In *Electron Transfer in Chemistry*, vol. **2**, Balzani V (ed). Wiley-VCH: Weinheim, 2001; 5–54.
2. (a) Knapp W, Tullius TD. *Chem. Rev.* 1998; **98**: 1089–1107; (b) Burrows CJ, Muller JG. *Chem. Rev.* 1998; **98**: 1109–1151.
3. (a) Newcomb M, Miranda N, Huang X, Crich D. *J. Am. Chem. Soc.* 2000; **122**: 6128–6129; (b) Müller SN, Batra R, Senn M, Giese B, Kisel M, Shadyro O. *J. Am. Chem. Soc.* 1997; **119**: 2795–2803.
4. (a) Stubbe J, Van der Donk WA. *Chem. Rev.* 1998; **98**: 705–762; (b) Smith DM, Golding BT, Radom L. *J. Am. Chem. Soc.* 2001; **123**: 1664–1675; (c) Smith DM, Golding BT, Radom L. *J. Am. Chem. Soc.* 2001; **121**: 5700–5704.
5. Abend A, Bandarian V, Reed GH, Frey PA. *Biochemistry* 2000; **39**: 6250–6257.
6. Schmittel M, Baumann U. *Angew. Chem.* 1990; **102**: 571–572; *Angew. Chem., Int. Ed. Engl.* 1990; **29**: 541–543.
7. Schmittel M, Röck M. *Angew. Chem.* 1994; **106**: 2056–2058; *Angew. Chem., Int. Ed. Engl.* 1990; **23**: 1961–1963.
8. Hart H, Rappoport Z, Biali SE. In *The Chemistry of Enols*, Patai S, Rappoport Z (eds). Wiley: Chichester, 1990; 481–589.
9. Rappoport Z, Biali SE. *Acc. Chem. Res.* 1988; **21**: 442–449.
10. Hegarty AF, O'Neill P. In *The Chemistry of Enols*, Patai S, Rappoport Z (eds). Wiley: Chichester, 1990; 639–650.
11. Harris RK (ed). *Nuclear Magnetic Resonance Spectroscopy*. Longman: Harlow, 1986; 204.
12. (a) Biali SE, Rappoport Z. *J. Am. Chem. Soc.* 1984; **106**: 5641–5653; (b) Rappoport Z, Nugiel DA, Biali SE. *J. Org. Chem.* 1988; **53**: 4814–4821.
13. Nadler EA, Rappoport Z. *J. Am. Chem. Soc.* 1989; **111**: 213–223.
14. Schmittel M, Gescheidt G, Eberson L, Trenkle H. *J. Chem . Soc., Perkin Trans. 2* 1997; 2145–2150.
15. Schmittel M, Langels A. *J. Chem . Soc., Perkin Trans. 2* 1998; 565–572.
16. Schmittel M, Keller M, Burghart A, Rappoport Z, Langels A. *J. Chem. Soc., Perkin Trans. 2* 1998; 869–875.
17. Nicholson RS, Shain I. *Anal. Chem.* 1964; **36**: 706–723.
18. Politzer P, Abu-Awwad F. *Theor. Chem. Acc.* 1998; **99**: 83–87.
19. Röck M, Schmittel M. *J. Chem. Soc., Chem. Commun.* 1993; 1739–1741.
20. Schmittel M, Gescheidt G, Röck M. *Angew. Chem., Int. Ed. Engl.* 1994; **33**: 1961–1963.
21. Fuson RC, Corse J, McKeever CH. *J. Am. Chem. Soc.* 1940; **62**: 3250
22. (a) Sheldrick GM. *SHELXs-97, a programme for Crystal Solution*. University of Göttingen: Göttingen, 1997; (b) Sheldrick GM. *SHELXL-97-2, a programme for Refinement of Crystal Structures*. University of Göttingen: Göttingen, 1997.